The impact of chlorine chemistry combined with heterogeneous N_2O_5 reactions on air quality in China

Xiajie Yang[1,2], Qiaoqiao Wang[1,2], Nan Ma[1,2], Weiwei Hu[3], Yang Gao[4], Zhijiong Huang[1,2], Junyu Zheng[1,2], Bin Yuan[1,2], Ning Yang[1,2], Jiangchuan Tao[1,2], Juan Hong[1,2], Yafang Cheng[5], Hang Su[5]

[1] Institute for Environmental and Climate Research, Jinan University, Guangzhou 511443, China.

[2] Guangdong-Hongkong-Macau Joint Laboratory of Collaborative Innovation for Environmental Quality, Guangzhou 511443, China.

[3] Guangzhou Institute of Geochemistry, Chinese Academy of Sciences, Guangzhou 510640, China.

[4] Key Laboratory of Marine Environment and Ecology, Ministry of Education, Ocean University of China, Qingdao 266100, China

[5] Max Planck Institute for Chemistry, Mainz 55128, Germany

Correspondence to: Qiaoqiao Wang (qwang@jnu.edu.cn)

Abstract: The heterogeneous reaction of N_2O_5 on Cl-containing aerosols ($N_2O_5 - ClNO_2$ chemistry) plays a key role in chlorine activation, NO_x recycling and consequently O_3 formation. In this study, we use the GEOS-Chem model with additional anthropogenic and biomass burning chlorine emissions combined with updated parameterizations for $N_2O_5 - ClNO_2$ chemistry (i.e. the uptake coefficient of N_2O_5 (γ_{N2O5}) and the $ClNO_2$ yield (φ_{ClNO2})) to investigate the impacts of chlorine chemistry on air quality in China, the role of $N_2O_5 - ClNO_2$ chemistry, as well as their sensitivities to chlorine emissions and parameterizations for γ_{N2O5} and φ_{ClNO2}. The model evaluation with multiple data sets observed across China demonstrated significant improvement especially regarding the simulation of Cl^-, N_2O_5 and $ClNO_2$ with the updates in chlorine emissions and $N_2O_5 - ClNO_2$ chemistry. Total tropospheric chlorine chemistry could increase annual mean MDA8 O_3 by up to 4.5 ppbv but decrease $PM_{2.5}$ by up to 7.9 µg m^{-3} in China, 83% and 90% of which could be attributed to the effect of $N_2O_5 - ClNO_2$ chemistry. The heterogeneous uptake of N_2O_5 on chloride-containing aerosol surfaces is an important loss pathway of N_2O_5 as well as a important source of O_3, and hence is particularly useful in elucidating the commonly seen ozone underestimations. The importance of chlorine chemistry largely depends on both chlorine emissions and the parameterizations for $N_2O_5 - ClNO_2$ chemistry. With the additional chlorine emissions annual mean maximum daily 8-hour average (MDA8) O_3 in China could be increased by up to 3.5 ppbv. The corresponding effect on $PM_{2.5}$ concentrations varies largely with regions, with an increase of up to 4.5 µg m^{-3} in the North China Plain but a decrease of up to 3.7 µg m^{-3} in the Sichuan Basin. On the other hand, even with the same chlorine emissions, the effects on MDA8 O_3 and $PM_{2.5}$ in China could differ by 48% and 27%, respectively between different parameterizations.

1 Introduction

35 Chlorine (Cl) plays an important role in atmospheric chemistry in both the stratosphere and the

36 troposphere, primarily via the reactions of Cl atom with various atmospheric trace gases including

37 dimethyl sulfide, methane, and other volatile organic compounds (VOCs). The chemistry of Cl is quite

38 similar with that of hydroxyl radicals (OH) while Cl atom reacts up to 2 orders of magnitude faster with

39 some VOCs than OH (Atkinson et al., 2006). Studies have shown that Cl accounts for around 2.5% –

40 2.7% of the global CH_4 oxidation in the troposphere, and the contribution varies across regions, reaching

41 up to 10% – 15% in Cape Verde and ~20% in east China (Lawler et al., 2011; Hossaini et al., 2016). Cl

42 atom, therefore, is regarded as a potentially important tropospheric oxidant.

43 In general, Cl atom can be produced from the photo-dissociation and the oxidation of chlorinated

44 organic species (e.g. CH_3Cl, CH_2Cl_2 and $CHCl_3$) and inorganic chlorine species (i.e. HCl and Cl_2).

45 Recently, nitryl chloride ($ClNO_2$), formed through the heterogeneous reaction between dinitrogen

46 pentoxide (N_2O_5) and chloride-containing aerosols, is found to be another important source of

47 tropospheric Cl atoms in polluted regions (Liu et al., 2018; Haskins et al., 2019; Choi et al., 2020). The

48 heterogeneous formation of $ClNO_2$ and the consequent photolysis can be described by reactions R1 –

49 R4 shown below (Finlayson-Pitts et al., 1989; Osthoff et al., 2008). The net reactions of R1 (N_2O_5

50 hydrolysis on none-chloride-containing aerosols) and R2 (uptake of N_2O_5 on chloride-containing

51 aerosols) could be expressed as R3, in which the $ClNO_2$ yield (i.e. φ_{ClNO2}, defined as the molar ratio of

52 produced $ClNO_2$ to total reacted N_2O_5) represents the fraction of N_2O_5 reacting via R2.

53 $N_2O_5 (g) + H_2O (aq) \rightarrow 2\ HNO_3 (aq)$ (R1)

54 $N_2O_5 (g) + HCl (aq) \rightarrow HNO_3 (aq) + ClNO_2 (g)$ (R2)

55 $N_2O_5 (g) + (1-\varphi)\ H_2O (aq) + \varphi\ HCl (aq) \rightarrow$

56 $(2-\varphi)\ HNO_3 (aq) + \varphi\ ClNO_2 (g)$ (R3)

57 $ClNO_2 (g) + h\nu \rightarrow Cl (g) + NO_2 (g)$ (R4)
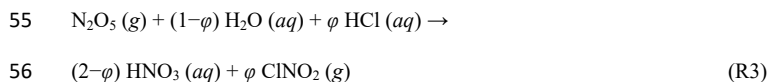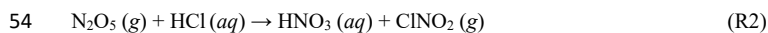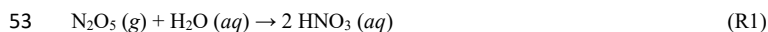
58 Estimates based on model simulations have suggested that $ClNO_2$ provides a source of Cl atoms totaling

59 0.66 Tg Cl a^{-1}, with the vast majority (95%) being in the Northern Hemisphere. The relative contribution

60   of ClNO$_2$ to global tropospheric Cl atoms is 14% on average and exhibits clear regional variations

61   (Sherwen et al., 2016). For example, the study by Riedel et al. (2012) reported that the relative

62   contribution is approximately 45% in Los Angeles based on a simple box model combined with local

63   observations.

64   The heterogeneous formation of ClNO$_2$ also serves as a reservoir for reactive nitrogen at night. The rapid

65   photolysis of ClNO$_2$ at daytime (R4) not only releases highly reactive Cl atom but also recycles NO$_2$ back

66   to the atmosphere, which as well significantly affect the daytime photochemistry (Thornton et al., 2010;

67   Riedel et al., 2014). It was suggested that the heterogeneous reaction between N$_2$O$_5$ and chloride-

68   containing aerosol could increase monthly mean values of the maximum daily 8h average (MDA8) O$_3$

69   concentrations by 1.0 – 8.0 ppbv in most Northern Hemisphere regions (Sarwar et al., 2014; Wang et al.,

70   2019). The reaction also impacts secondary aerosol formation, mainly through the recycling of NO$_x$

71   (Staudt et al., 2019; Mitroo et al., 2019). For example, Sarwar et al. (2014) estimated that ClNO$_2$

72   production decreases nitrate by 3.3% in winter and 0.3% in summer averaged over the entire Northern

73   Hemisphere. The influence of the heterogeneous formation of ClNO$_2$ in China is even larger due to the

74   polluted environment, leading to an increase in ozone concentrations by up to 7 ppbv, and a decrease in

75   total nitrate by up to 2.35 µg m^{-3} on monthly mean basis (Li et al., 2016; Sarwar et al., 2014)

76   There are two key parameters determining the heterogeneous uptake of N$_2$O$_5$, including the uptake

77   coefficient of N$_2$O$_5$ (γ_{N2O5}) and the ClNO$_2$ yield (φ_{ClNO2}). The most widely used parameterization for γ_{N2O5}

78   and φ_{ClNO2} was proposed by Bertram and Thornton (2009), which is based on the laboratory studies with

79   considerations of temperature, relative humidity (RH), aerosol water content, concentrations of nitrate

80   and chloride, and specific surface area. However, recent field and model studies have shown that this

81   parameterization would overestimate both γ_{N2O5} and φ_{ClNO2}, especially in regions with high Cl levels

82   (Mcduffie et al., 2018b; Mcduffie et al., 2018a; Xia et al., 2019; Chang et al., 2016; Hong et al., 2020;

83   Yu et al., 2020). The discrepancies could be partly attributed to the complexity of atmospheric aerosols

84   (e.g. mixing state and complex coating materials) in contrast to the simple proxies used in laboratory

85   studies (Yu et al., 2020). Several parameterizations updated from the one by Bertram and Thornton (2009)

86   have been proposed by more recent studies based on field measurements and box model studies (Yu et

87   al., 2020; Mcduffie et al., 2018a; Mcduffie et al., 2018b; Xia et al., 2019). However, a full evaluation of

88 the representativeness of different parameterizations for the $N_2O_5 - ClNO_2$ chemistry and the associated

89 impacts on ambient air quality is not available yet.

90 In addition to the parameterization, the influence of the $N_2O_5 - ClNO_2$ chemistry is also sensitive to

91 chlorine emissions. In early modelling studies, global tropospheric chlorine is mainly from sea salt

92 aerosols (SSA), and most of the chlorine over continental regions in North America and Europe is

93 dominated by the long-range transport of SSA (Wang et al., 2019; Sherwen et al., 2017). The importance

94 of anthropogenic chlorine emissions, which were ignored in most studies, has been raised recently based

95 on both field measurements and model simulations (Le Breton et al., 2018; Yang et al., 2018; Wang et

96 al., 2020; Hong et al., 2020). The study by Wang et al. (2020b) suggested that anthropogenic emissions

97 could dominate reactive chlorine in China, resulting in an increase in $PM_{2.5}$ and Ozone by up to 3.2 µg

98 m^{-3} and 1.9 ppbv on annual mean basis, respectively. The comprehensive effects of anthropogenic

99 chlorine on air quality as well as their sensitivities to different parameterizations for $N_2O_5 - ClNO_2$

100 chemistry, however, has not been investigated in previous studies.

101 In this work, we use the GEOS-Chem model to investigate the impacts of chlorine chemistry including

102 the heterogeneous $N_2O_5 - ClNO_2$ chemistry on air quality in China. Multiple observational data sets,

103 including N_2O_5, $ClNO_2$, O_3, $PM_{2.5}$ and its chemical species from different representative sites across

104 China, are used to assess the model performance. With comprehensive chlorine emissions as well as

105 appropriate parameterizations for $N_2O_5 - ClNO_2$ chemistry, our objectives are: 1) to improve the model's

106 performance regarding the simulation of particulate chloride, $ClNO_2$, N_2O_5, $PM_{2.5}$ and O_3 concentrations;

107 and 2) to extend the investigation on the effects of chlorine chemistry on both $PM_{2.5}$ and ozone pollution

108 in China as well as their sensitivities to anthropogenic chlorine emissions and the parameterizations for

109 $N_2O_5 - ClNO_2$ chemistry.

110 **2 Methodology**

111 **2.1 GEOS-Chem Model**

112 The GEOS-Chem model (version 12.9.3, http://www.geos-chem.org) is driven by assimilated

113   meteorological fields GEOS-FP from the NASA Global Modeling and Assimilation Office (GMAO) at

114   NASA Goddard Space Flight Center. The simulation in this study was conducted in a nested-grid model

115   with a native horizontal resolution of $0.25° \times 0.3125°$ (latitude $\times$ longitude) and 47 vertical levels over

116   East Asia ($70° - 140°$ E, $15°$ S $- 55°$ N). The dynamical boundary conditions were from a global simulation

117   with a horizontal resolution of $2° \times 2.5°$. We initialized the model with a 1-month spin up followed by a

118   1-year simulation for 2018. The simulation included a detailed representation of coupled NO_x – ozone –

119   VOCs – aerosol − halogen chemistry (Sherwen et al., 2016). Previous studies have demonstrated the

120   ability of GEOS-Chem to reasonably reproduce the magnitude and seasonal variation of surface ozone

121   and particulate matter over East Asia and China (Wang et al., 2013; Geng et al., 2015; Li et al., 2019).

122   **2.1.1 Chlorine Chemistry**

123   The GEOS-Chem model includes a comprehensive chlorine chemistry mechanism coupled with bromine

124   and iodine chemistry. Full details could be found in the study of Wang et al. (2019b). Briefly, the model

125   includes 12 gas-phase inorganic chlorine species (Cl, Cl_2, Cl_2O_2, $ClNO_2$, $ClNO_3$, ClO, ClOO, OClO,

126   BrCl, ICl, HOCl, HCl), 3 gas-phase organic chlorine (CH_3Cl, CH_2Cl_2, $CHCl_3$), and aerosol Cl^- in two

127   size bins (fine mode with radius $\leqslant$ 0.5 μm and coarse mode with radius > 0.5 μm). The gas-aerosol

128   equilibrium between HCl and Cl^- is calculated with ISORROPIA II (Fountoukis and Nenes, 2007) as

129   part of the $H_2SO_4 - HCl - HNO_3 - NH_3$ – non-volatile cations (NVCs) thermodynamic system, where

130   Na^+ is used as a proxy for NVCs.

131   The heterogeneous uptake of N_2O_5 on aerosol surfaces leading to the production of $ClNO_2$ and HNO_3

132   has also been included in GEOS-Chem with parameterizations for γ_{N2O5} and φ_{ClNO2} proposed by McDuffie

133   et al. (2018b; 2018a) by default (hereinafter referred to as McDuffie Parameterization). The γ_{N2O5} can be

134   described by Eq. 1:

135
$$\frac{1}{\gamma_{N_2O_5}} = \frac{1}{\gamma_{core}} + \frac{1}{\gamma_{coat}}$$
Eq. 1

136   Where γ_{core} represents the reactive uptake of inorganic aerosol core, and γ_{coat} represents the retardation of

137   the organic coating. More details of the parameterization can be referred to McDuffie et al. (2018b).

138   φ_{ClNO2} is calculated following the study of Bertram and Thornton (2009), but is reduced by 75% based

139   on the observations conducted in eastern U.S. and offshore in spring 2015 (Lee et al., 2018). It could be

140   described by Eq. 2:

141    $$\varphi_{\text{ClNO}_2} = 0.25 \times \left(\frac{k_2[\text{H}_2\text{O}]}{k_3[\text{Cl}^-]} + 1 \right)^{-1} \qquad \text{Eq. 2}$$

142   Where [H_2O] and [Cl^-] are the concentrations of aerosol liquid water content and aerosol chloride,

143   respectively, and $k_3/k_2 = 450$. The McDuffie parameterization can reproduce observed mean values of

144   γ_{N2O5} and φ_{ClNO2} in eastern U.S. (Mcduffie et al., 2018b; Mcduffie et al., 2018a), but is still of great

145   uncertainty.

146   Recently, Yu et al. (2020) proposed new parameterizations of γ_{N2O5} and φ_{ClNO2} based on the direct

147   measurements at two sites in northern and southern China representing different atmospheric conditions.

148   The parameterizations (hereinafter referred to as Yu Parameterization) are described by Eq. 3 − 4:

149    $$\gamma_{\text{N}_2\text{O}_5} = 6.12 \times 10^6 \times \frac{[\text{H}_2\text{O}]V}{c \cdot S_a} \left(1 - \frac{1}{0.033 \times \frac{[\text{H}_2\text{O}]}{[\text{NO}_3^-]} + 3.4 \times \frac{[\text{Cl}^-]}{[\text{NO}_3^-]} + 1} \right) \quad \text{Eq. 3}$$

150    $$\varphi_{\text{ClNO}_2} = \left(1 + \frac{[\text{H}_2\text{O}]}{105[\text{Cl}^-]} \right)^{-1} \qquad \text{Eq. 4}$$

151   Where c is an average gas-phase thermal velocity of N_2O_5; V and S_a are particle volume and surface area

152   densities, respectively; [H_2O], [Cl^-] and [NO_3^-] are the concentrations of aerosol liquid water content,

153   aerosol chloride and aerosol nitrate, respectively.

154   In this study, we updated the N_2O_5 − ClNO_2 chemistry in GEOS-Chem with the Yu parameterization.

155   Additional simulation cases were also performed to evaluate the representativeness of both the Yu and

156   McDuffie Parameterizations regarding the simulation of N_2O_5, ClNO_2, O_3, $\text{PM}_{2.5}$ and its chemical

157   speciation in China. Detailed description of the model setup for related cases is provided below in Section

158   2.1.3.

159   **2.1.2 Emissions**

160   The study uses the Hemispheric Transport of Air Pollution (HTAPv2, http://www.htap.org/) based on the

161   emission of 2010 as a global anthropogenic inventory. This inventory is overwritten by a regional

162   emission inventory MIX (with a horizontal resolution of $0.25° \times 0.25°$) over East Asia based on the

163   emission in 2017, which is developed for the Model Inter-Comparison Study for Asia (MICS-Asia) and

164   covers all major anthropogenic sources in 30 Asian countries and regions (Li et al., 2017). In addition,

165   anthropogenic emissions of black carbon (BC) and organic carbon (OC) in Guangdong province, China

166    $(109° - 117°$ E, $20° - 26°$ N) are overwritten by a more recent high-resolution inventory (9 km × 9 km)

167   described by Huang et al. (2021). Biomass burning emissions are from the Global Fire Emissions

168   Database (GFED4) (Van et al., 2010) with a 3-hour time resolution. And the biogenic emissions of VOCs

169   are calculated based on the Model of Emissions of Gases and Aerosols from Nature (MEGAN2.1)

170   (Guenther et al., 2006).

171   Table 1 lists Cl emissions from all sources in the model. The global tropospheric chlorine by default in

172   the model is mainly from the mobilization of Cl^- from SSA distributed over two size bins (fine and coarse

173   modes) (Wang et al., 2019), which is computed online as the integrals of the size-dependent source

174   function depending on wind speeds and sea surface temperatures (Jaeglé et al., 2011). During the

175   simulation year of 2018, SSA contributes 6.5×10^4 Gg Cl^-, most of which however are distributed over

176   the ocean due to its relatively short lifetime (∼1.5 days) (Choi et al., 2020). The release of atomic Cl

177   from organic chlorine (CH_3Cl, CH_2Cl_2 and $CHCl_3$) via the oxidation by OH and Cl is also included in

178   the model by default. These organic chlorine gases are mainly of biogenic marine origin (Simmonds et

179   al., 2006), with a mean tropospheric lifetime longer than 250 days (Wang et al., 2020), and are simulated

180   in the model by imposing fixed surface concentrations as described by Schmidt et al. (2016). Total

181   emissions of Cl atom from CH_3Cl, CH_2Cl_2, and $CHCl_3$ are estimated to be 3.8, 2.4, and 0.70 Gg Cl a^{-1},

182   respectively.

183   Considering the importance of anthropogenic chlorine in China, we have further updated chlorine

184   inventories in the model to account for anthropogenic HCl, Cl_2 and fine particulate Cl^-, as well as biomass

185   burning HCl and Cl^- emissions (also shown in Table 1). For fine particulate Cl^- from both anthropogenic

186   and biomass burning, the emissions are estimated based on $PM_{2.5}$ emissions from MIX and GFED4

187   inventories combined with the emission ratios of fine particulate Cl^- versus $PM_{2.5}$ for different emission

188   sectors adopted from the study of Fu et al. (2018). Estimated Cl^- emissions from anthropogenic and

189   biomass burning are 379 and 120 Gg, respectively, comparable to the results of 486 Gg in total for the

190   year of 2014 by Fu et al. (2018). The anthropogenic emissions of HCl and Cl_2 are from ACEIC

191   (Anthropogenic Chlorine Emissions Inventory for China) (Liu et al., 2018) and are estimated to be 218

192   and 8.9 Gg Cl in China, respectively. For HCl from biomass burning, the emission factors from Lobert

193   et al. (1999) are used for different types of biomass provided in GFED4, and a total emission of 30 Gg

194   Cl is obtained in China in 2018. Total implemented chlorine emission for the simulation year of 2018 is

195   756 Gg Cl.

196   Figure 1 shows the distribution of Cl emissions from the sources mentioned above. Anthropogenic and

197   biomass burning emissions of HCl are concentrated in the Northeast Plain (NP), North China Plain (NCP),

198   Yangtze River Delta (YRD), and Sichuan Basin (SCB), and could be up to 320 kg Cl km^{-2} a^{-1} in the SCB.

199   Emissions of HCl are low in South China, mainly due to the low chlorine content of coal in these regions

200   (Hong et al., 2020). The relative contribution of biomass burning to total HCl emissions in China is 14%

201   on average, but could become dominant in the NP due to the discrepancies in the spatial distributions of

202   anthropogenic and biomass burning emissions. The anthropogenic Cl$_2$ emissions have a similar spatial

203   distribution to that of HCl, but are one order of magnitude lower than HCl emissions. The distribution of

204   non-sea salt Cl$^-$ emissions is also similar to that of HCl and Cl$_2$, except that non-sea salt Cl$^-$ emissions

205   are also high in Central China. In contrast, emissions of sea salt Cl$^-$ (Fig. S1) are mainly distributed over

206   the ocean, implying limited influences over inland due to rapid deposition during transport. The spatial

207   distributions of different organic chlorine sources are similar, with maximums (~ 0.5 kg Cl km^{-2} a^{-1}) in

208   coastal regions (Fig. S1).

209   **2.1.3 Model setup for different simulation cases**

210   In this study, we conducted a series of simulation cases to investigate the effects of chlorine chemistry

211   on air quality in China, the role of N$_2$O$_5$ − ClNO$_2$ chemistry, and the associated sensitivities to chlorine

212   emissions as well as the parameterizations for N$_2$O$_5$ − ClNO$_2$ chemistry. Detailed model setup for those

213   cases is listed in Table 2. The Base case is the one with all updates in this study, including additional

214   chlorine sources from anthropogenic and biomass burning emissions as well as improved N$_2$O$_5$ − ClNO$_2$

215   chemistry represented by the Yu parameterization. The NoEm case is conducted with a similar setup as

216   the Base case but only includes chlorine emissions from SSA and organic chlorine sources so as to

217   evaluate the model improvement originated from the updated chlorine emissions through the comparison

218   with the Base case. The McDuffie case is also performed using the McDuffie instead of Yu

219   parameterization for γ_{N2O5} and φ_{ClNO2} while keeping others the same as the Base case so as to evaluate the

220   discrepancies originated from different parameterizations for the N$_2$O$_5$ − ClNO$_2$ chemistry.

221   In addition, the NoHet case sets φ_{ClNO2} to zero (i.e. [Cl$^-$] = 0 in Eq. 3 and 4) but keeps others the same as

222   the Base case so as to evaluate the importance of the of $N_2O_5 - ClNO_2$ chemistry through the comparison

223   with the Base case. Similarly, combined with three more sensitivity cases (NoChem, NoEmHet and

224   NoAll, see details in Table 2), the study provides an overall evaluation of the importance of tropospheric

225   chlorine chemistry as well as its sensitivities to chlorine emissions and the parameterizations for $N_2O_5 -$

226    $ClNO_2$ chemistry in the model.

227   **2.2 Observations**

228   Multiple observed data sets were applied in this study to evaluate the performance of GEOS-Chem

229   simulation, including the concentrations of chemical species of $PM_{2.5}$ from three representative sites,

230   located in south (Guangzhou, 23.14° N, 113.36° E), east (Dongying, 37.82° N, 119.05° E) and north

231   (Gucheng, 37.36° N, 115.96° E) China, respectively (Fig. S2). Concentrations of SO_4^{2-}, NO_3^-, NH_4^+, Cl^-

232   and organic matter (OM) in $PM_{2.5}$ were measured by High Resolution Time-of-Flight Aerosol Mass

233   Spectrometer (HR-ToF-AMS; Aerodyne Research Inc., USA, Decarlo et al. (2006)) from October 2 to

234   November 18, 2018 (with a time resolution of 1 minute) at Guangzhou site (Chen et al., 2021b), and

235   from March 18 to April 21, 2018 (with a 1-minute time resolution) at Dongying site. Concentrations of

236   these species were measured by an Aerodyne Quadruple Aerosol Chemical Speciation Monitor (ACSM;

237   Aerodyne Research Inc., USA, Ng et al. (2011)) from November 11 to December 18 in 2018, with a time

238   resolution of 2 minutes at Gucheng site (Li et al., 2021).

239   Concentrations of N_2O_5 and $ClNO_2$ (with a time resolution of 1 minute) were also measured at

240   Guangzhou site by a Chemical Ionization Mass Spectrometer (CIMS, THS Instruments Inc., Atlanta,

241   (Kercher et al., 2009)) from September 25 to November 12 in 2018 (Ye et al., 2021). To have a thorough

242   evaluation of the representativeness of different parameterizations for γ_{N2O5} and φ_{ClNO2}, observations of

243    $ClNO_2$ and N_2O_5 at six more sites across China from previous studies (see Table S1 and Fig. S2) are also

244   used in this study. It should be noted that model results sampled at those sites for comparison were

245   simulated in the same months but different years while ignoring the uncertainties associated with the

246   interannual variability.

247   In addition, we also use observed hourly data of O_3 and $PM_{2.5}$ published by the China National

248   Environmental Monitoring Center (CNEMC, http://www.cnemc.cn/sssj/, last access on June 20, 2021)

249   to evaluate the model's overall performance in China. The network was launched in 2013 as part of the

250   Clean Air Action Plan, and includes ∼1500 stations located in 370 cities by 2018 (Fig. S2).

251   **3 Results and discussion**

252   **3.1 Improved model performance with updated chlorine emissions and $N_2O_5 - ClNO_2$ chemistry**

253   Figure 2 shows time series of observed and simulated Cl^- concentrations at the Guangzhou, Dongying,

254   and Gucheng sites. The observations show the lowest Cl^- concentrations at the Guangzhou site ($0.55 \pm$

255   0.52 µg m^{-3}), although the site is the closest to the ocean among all three sites, while the highest

256   concentrations (4.7 ± 3.3 µg m^{-3}) are observed at the Gucheng site, away from the sea. Moderate

257   concentrations of Cl^- is observed at the Dongying site, around 1.1 ± 0.82 µg m^{-3}. The relatively higher

258   concentrations observed inland again suggest the dominance of non-sea salt Cl^- in China, as mentioned

259   before in the Introduction.

260   The comparison between observations and simulated results from the NoEm case shows a serious

261   underestimate of Cl^- concentrations, with normalized mean bias (NMB) ranging from -96% to -79%,

262   suggesting the missing of significant chlorine sources in addition to sea salt chlorine. In contrast, the

263   Base case with updated chlorine emissions exhibits much higher Cl^- concentrations and can successfully

264   reproduce observations, with average of 0.77 ± 0.54, 0.71 ± 0.52, and 4.5 ± 2.4 µg m^{-3} at the Guangzhou,

265   Dongying, and Gucheng sites, respectively. The increase in Cl^- concentrations in the Base case compared

266   with the NoEm case is the most significant at the Gucheng site, by a factor of 24 (from 0.19 to 4.5 µg m$^-$

267   ^{3} on average). The NMB in the Base case therefore has decreased to -36% – 39%. The slight

268   underestimates at the Dongying site in the Base case could be to some extent explained by the bias in

269   GFED4, which underestimates emissions from agricultural fires due to their small size and short duration

270   as suggested by the study of Zhang et al. (2020). In spite of that, the model with the Base case well

271   reproduces the overall distribution of the observed particulate chloride concentrations in China. The

272   correlation coefficients (r) between observed and model results at the three sites also increase from -0.05

273   – 0.61 in the NoEm case to 0.40 – 0.71 in the Base case. The significant improvement in the model

274   performance again suggests sources other than SSA play a key role in Cl$^-$ concentrations in China.

275   The comparison between observed and simulated N_2O_5 (Fig. 3a) shows that NMB for the NoEm case are

276   -58%, 150%, 108% and 25% at the Guangzhou, Wangdu, Taizhou and Mount Tai sites, respectively. In

277   contrast, the corresponding NMB for the Base case are much smaller, -57%, 48%, 91% and 18%,

278   respectively. The improvement in the Base case is apparent at most sites, implying that additional

279   chlorine emissions combined with the updated $N_2O_5 - ClNO_2$ chemistry with Yu parameterization could

280   effectively increase the uptake coefficient of N_2O_5. Little improvement is found at the Guangzhou site (-

281   58% in the NoEm case vs. -57% in the Base case). Previous studies also found an underestimation of

282   N_2O_5 in the Pearl River Delta (PRD), which could be partly explained by the underestimation of the

283   sources (e.g NO_2) and/or the overestimation of the sink of N_2O_5 there (Dai et al., 2020; Li et al., 2016).

284   The N_2O_5 results from the McDuffie case, which uses the McDuffie parameterization (a default setting

285   in GEOS-Chem, see Section 2.1.1 and 2.1.3) instead of Yu parameterization are also shown in Fig. 3a.

286   The NMB for the McDuffie case are -53%, 154%, 143% and 37% at the Guangzhou, Wangdu, Taizhou

287   and Mount Tai sites, respectively. The comparison indicates that Yu parameterization can reproduce

288   observed N_2O_5 better in China in general, while McDuffie parameterization tends to overestimate N_2O_5

289   concentrations, which could be attributed to the suppression from the organic coatings leading to a much

290   lower γ_{N2O5} (see Eq. 1 for McDuffie parameterization). Similarly, Morgan et al. (2015) found significant

291   underestimates in γ_{N2O5} when the effect of organic coatings is considered. The effect of organic coatings

292   strongly depends on organic composition, particle phase state, and the environmental factors (e.g. RH

293   and temperature), and thus remains poorly quantified (Mcduffie et al., 2018b; Morgan et al., 2015). As

294   suggested by the study of Yu et al. (2020), the bias in γ_{N2O5} in McDuffie parameterization could be to

295   some extent explained by the fact that the parameterization does not differentiate between water-soluble

296   and water-insoluble organic fractions and simplifies the morphology and phase state, resulting in an

297   underestimation of the solubility and the diffusivity of N_2O_5 in organic matter.

298   For the comparison of $ClNO_2$ (Fig. 3b), we use the mean nighttime (excluding the data at local time of

299   10:00 – 16:00) maximum mixing ratio, as suggested by Wang et al. (2019b and 2020b). Observed $ClNO_2$

300   is high in Guangzhou (1121 pptv) and Wangdu (~ 990 pptv), followed by Changping (~ 500 pptv) and

301   Beijing (~ 430 pptv). The lowest concentrations are obtained at Mount Tai and Mount TaiMoShan (~ 150

302 and 120 pptv, respectively) due to relatively clean condition at high altitude. The comparison between

303 observed and simulated $ClNO_2$ at different sites also suggests a better model performance for the Base

304 case with NMB in the range of -28% – 22%, compared with the NMB of -77% – -31% and -59% – -36%

305 for the NoEm and McDuffie cases, respectively. The large difference between the NoEm and Base cases

306 again emphasizes the important role of non-sea salt chlorine in the formation of $ClNO_2$. The

307 underestimates in McDuffie parameterization on the other hand may suggest that the scaling factor of

308 0.25 applied to φ_{ClNO2} in Eq. 2 is not appropriate for the atmospheric condition in China. A scaling factor

309 of 0.5 instead of 0.25 may fit better with observations used in the study. More field measurements and

310 model evaluations are required to come up with a more precise scaling factor better representing φ_{ClNO2}

311 in China. Overall, with updated chlorine emissions and Yu parameterization for γ_{N2O5} and φ_{ClNO2}, the Base

312 case agrees better with both the magnitude and the spatial variation of observed N_2O_5 and $ClNO_2$ in

313 China.

314 To further elucidate how the model behaves in reproducing the spatial distribution of ozone and $PM_{2.5}$

315 through the incorporation of the additional chlorine emissions and updated $N_2O_5 − ClNO_2$ chemistry with

316 Yu parameterization, simulated MDA8 O_3 and $PM_{2.5}$ from different cases were compared with

317 observations across China. Figure 4 shows observed annual mean MDA8 O_3 and $PM_{2.5}$ in 2018 in China

318 from CNEMC compared with the model results from the Base case. The observed annual mean MDA8

319 O_3 and $PM_{2.5}$ are 49 ppbv and 39 $\mu g\ m^{-3}$ respectively in 2018 in China. Model results from the Base case

320 could generally reproduce observed spatial and seasonal variations of annual mean MDA8 O_3 and $PM_{2.5}$

321 concentrations, with NMB of -26% and 3.6% and r of 0.83 and 0.81 respectively.

322 Table 3 also summarized the model performance on both annual and seasonal scales regarding the

323 simulation of O_3 and $PM_{2.5}$ from different cases. For the comparison with observed MDA8 O_3, although

324 different simulation cases show a similar range of r, the Base case tends to have a slightly smaller bias

325 in general, with NMB of -26% on annual average (-49% – -5.5% on seasonal mean) vs. -28% (-54% – -

326 5.9%) in the NoEm and -27% (-53% – -5.2%) in the McDuffie case. For the comparison with observed

327 $PM_{2.5}$, the NMB bias from the Base case is 3.6% on annual average (-6.3% – 28% on seasonal mean).

328 Compared with the NoEm case, there is some improvement in summer (5.0% vs. 3.9%) and winter (-

329 7.9% vs. -4.3%) but slightly larger bias in autumn (26% vs. 28%). The McDuffie case on the other hand

330   produces slightly higher PM$_{2.5}$ concentrations, with NMB of 5.6%. Regarding the simulation of

331   particulate chemical species (Table S2), although the model performance varies with sites and species,

332   the Base case demonstrates better agreement with observations compared with the NoEm and McDuffie

333   cases in general.

334   On the whole, the model performance is better with the additional anthropogenic and biomass burning

335   chlorine emissions combined with updated N$_2$O$_5$ − ClNO$_2$ chemistry represented by Yu parameterization.

336   Therefore, the following investigation of the impacts of chlorine chemistry on air quality in China as

337   well as their sensitivities to chlorine emissions and parameterizations for N$_2$O$_5$ − ClNO$_2$ chemistry is

338   mainly based on the Base case.

339   **3.2 Impacts of tropospheric chlorine chemistry on air quality and the role of N$_2$O$_5$ − ClNO$_2$**

340   **chemistry**

341   To comprehensively quantify the importance of chlorine chemistry, we conducted a sensitivity case in

342   which all related tropospheric chlorine chemistry was turned off (NoChem, also listed in Table 2). The

343   differences between the Base and NoChem cases (Fig. 5 and Fig. S3) could thus represent the impact of

344   the chlorine chemistry. The comparison shows that chlorine chemistry could increase annual mean

345   nighttime max ClNO$_2$ surface concentrations by 243 pptv averaged in China (up to 1548 pptv in the

346   SCB). The increase in annual mean Cl atoms is 1.7×10^3 molec cm^{-3} averaged in Chian (up to 7×10^3

347   molec cm^{-3} in coastal regions), which further lead to an increase in surface annual mean MDA8 O$_3$ and

348   OH by 1.1 ppbv and 3.8×10^4 molec cm^{-3} averaged in China (up to 4.5 ppbv and 1.2×10^5 molec cm^{-3} in

349   the SCB) respectively through VOCs oxidation. In contrast, annual mean PM$_{2.5}$ surface concentrations

350   are decreased by 0.91 μg m^{-3} averaged in China (up to 7.9 μg m^{-3} in the SCB), mainly due to the decrease

351   of NO$_3^-$ and NH$_4^+$ (up to 6.4 μg m^{-3} and 1.9 μg m^{-3} respectively), although SO$_4^{2-}$ concentrations are

352   increased slightly by up to 1.2 μg m^{-3} in the SCB (Fig. S3).

353   Previous studies suggested that tropospheric chlorine drives a global decrease of O$_3$ by catalytic

354   production of bromine and iodine radicals from hypohalous acids (HOX, where X = Br and I) (Schmidt

355   et al., 2016; Wang et al., 2019). On the contrary, N$_2$O$_5$ – ClNO$_2$ chemistry can enhance O$_3$ through the

356   production of Cl atoms and the recycling of NO$_x$. Therefore, we further investigate the role that N$_2$O$_5$ −

357 $ClNO_2$ chemistry plays in tropospheric chlorine chemistry through the comparison between the Base and

358 NoHet (Fig. 6 and Fig. S4). The comparison illustrates that the $N_2O_5 – ClNO_2$ chemistry could result in

359 a significant production of $ClNO_2$, reaching $600 – 1400$ pptv for annual mean nighttime max surface

360 concentrations in the NCP, and up to 1546 pptv in the SCB. The change in the surface concentrations of

361 Cl atoms (an annual mean increase of $1 – 4 \times 10^3$ molec cm^{-3} in central and eastern China) is mainly due

362 to the photolysis of $ClNO_2$ and accounts for 74% of total change in annual mean Cl atoms due to all

363 tropospheric chlorine chemistry in China, which are consistent with the results from the previous study

364 by Liu et al. (2017).

365 Consequently, the annual mean MDA8 O_3 surface concentrations are increased by $1.5 – 3$ ppbv in central

366 and eastern China and by up to 3.8 ppbv in the SCB, accounting for 83% of total change in annual mean

367 MDA8 O_3 due to all tropospheric chlorine chemistry in China. It is interesting to note that while MDA8

368 O_3 surface concentrations show maxima in summer and minima in winter in general, the influence of

369 $N_2O_5 – ClNO_2$ chemistry on O_3 concentrations exhibits a different seasonality. The increase in seasonal

370 mean MDA8 O_3 concentrations is the largest in winter (by up to 6.5 ppbv in the SCB), but is less than

371 1.5 ppbv in summer. This is because of more accumulation of N_2O_5 and $ClNO_2$ in dark conditions in long

372 winter nights (Sarwar et al., 2014).

373 There also exhibits an obvious decrease in the annual mean surface concentrations of $PM_{2.5}$ attributed to

374 the $N_2O_5 – ClNO_2$ chemistry, ranging from 1.5 to 4.5 µg m^{-3} in central and eastern China (accounting for

375 90% of total change in annual mean $PM_{2.5}$ due to all tropospheric chlorine chemistry in China). The

376 decrease is more significant in autumn and winter in China, with a range of $3.5 – 5.5$ µg m^{-3} in central

377 and eastern China, and being up to 11 µg m^{-3} in the SCB. In contrast, the decrease in $PM_{2.5}$ is less than 2

378 µg m^{-3} in summer in China. The change in $PM_{2.5}$ is mainly due to the decrease in NO_3^- (up to 6.2 µg m^{-3}

379 in the SCB on annual average). In addition, NH_4^+ is also decreased by up to 1.8 µg m^{-3} in the SCB on

380 annual average, following the pattern of ΔNO_3^-. This is because NH_3 is in excess in most regions in China

381 (Xu et al., 2019) and the formation of $ClNO_2$ via R2 could hinder the formation of HNO_3 and shift the

382 partitioning between NH_3 and NH_4^+ towards NH_3. Unlike the change in NO_3^- and NH_4^+, the $N_2O_5 – ClNO_2$

383 chemistry increases surface SO_4^{2-} concentration slightly, which could be explained by the enhancements

384 of atmospheric oxidation associated with the increase in Cl atoms, OH and O_3, facilitating the formation

385   of secondary aerosols (Sarwar et al., 2014).

386   On the other hand, the effect of tropospheric chlorine chemistry without the $N_2O_5 – ClNO_2$ chemistry is

387   much smaller (Fig. S5), leading to an increase of up to 0.7 ppbv in inland China and a decrease of 0.3 –

388   0.5 ppbv in coastal regions for annual mean MDA8 O_3 concentrations. The increase is probably

389   associated with Cl atoms from photolysis of gas-phase chlorine, especially non-sea salt Cl_2 in inland

390   China, while the decrease at coastal regions is mainly due to catalytic production of bromine and iodine

391   radicals originated from sea-salt aerosols. The comparison demonstrates the dominance of $N_2O_5 – ClNO_2$

392   chemistry in total tropospheric chlorine chemistry in China.

393   3.3 The effect of $N_2O_5 – ClNO_2$ chemistry in response to chlorine emissions

394   Since both γ_{N2O5} and φ_{ClNO2} in the Yu parameterization are highly dependent on [Cl⁻], the effect of N_2O_5

395   – $ClNO_2$ chemistry on air quality is thus sensitive to chlorine emissions. Figure 7 shows the effects of

396   additional chlorine emissions from anthropogenic and biomass burring sources on annual mean surface

397   concentrations of different species (Cl⁻, Cl atom, OH, MDA8 O_3, $PM_{2.5}$ and NO_3^-) in China, calculated

398   as the differences between the Base and the NoEm case. With the implementation of the additional

399   chlorine emissions, the particulate Cl⁻ concentration increased significantly in inland China, with the

400   largest increase in the SCB (4.5 µg m⁻³) and little change in west China. The increase is in the range of

401   1.5 – 3.5 µg m⁻³ in the NCP and < 0.5 µg m⁻³ in South China. The spatial distribution of ΔCl atoms is

402   also consistent with that of the additional chlorine emissions and ΔCl⁻, showing the largest increment in

403   the SCB (about $4.5 – 5 \times 10^3$ molec cm⁻³). There is also a moderate increase in Cl atoms in the NP and

404   NCP, with a range of $1.5 – 4 \times 10^3$ molec cm⁻³. Only a minor increase of Cl atoms is found in South China

405   ($< 1 \times 10^3$ molec cm⁻³).

406   The reactions of VOCs with Cl atoms lead to a further increase in OH (an annual mean increase of 2 – 9

407    $\times 10^4$ molec cm⁻³ in central and eastern China) and O_3 (Wang et al., 2016; Sarwar et al., 2014). The

408   increase in O_3 could also be due to the recycling of NO_x back to the atmosphere associated with the

409   photolysis of $ClNO_2$ (R4). The increase in MDA8 O_3 surface concentrations ranges from 0.5 to 3 ppbv

410   in central and eastern China, and reaches up to 3.5 ppbv in the SCB on annual average. The impacts of

411   chlorine sources on O_3 formation also vary with seasons. Although O_3 pollution is generally severe in

412   summer, the change in MDA8 O_3 due to chlorine sources is relatively minor, with maxima of 0.7 ppbv

413   in the SCB and < 0.5 ppbv in most other regions averaged in summer. In contrast, the increase is most

414   obvious in winter, with maxima of 5.2 ppbv in the SCB on seasonal average.

415   The effects of the additional chlorine emissions on surface $PM_{2.5}$ concentrations is complicated. The NCP

416   shows the largest increase (3 – 4.5 µg m^{-3} on annual average), mainly due to the increase in Cl^-, which

417   could also promote N_2O_5 – $ClNO_2$ chemistry and lead to more NO_3^- production (Chen et al., 2021a). In

418   contrast, the SCB exhibits both an increase (by up to 4.2 µg m^{-3}) and a decease (by up to 3.7 µg m^{-3}). The

419   decrease of $PM_{2.5}$ in the SCB is mainly due to the large decrease of NO_3^- there. In the SCB, nitrate

420   formation is dominated by the heterogeneous hydrolysis of N_2O_5 (Tian et al., 2019) while the additional

421   Cl^- could hinder the path of N_2O_5 hydrolysis due to competition with the path of $ClNO_2$ formation.

422   Consequently, the additional chlorine emissions result in a decrease of NO_3^- up to 5.6 µg m^{-3} in SCB on

423   annual average.

424   In addition, NH_4^+ concentrations could also be affected through the reaction of R5:

425    $HCl\,(g) + NH_3\,(g) \rightarrow NH_4^+ + Cl^-$ (R5)

426   In the NP and NCP where anthropogenic and biomass burning emissions of HCl are high, the annual

427   mean NH_4^+ surface concentrations are increased by 0.5 – 1.5 µg m^{-3} (Fig. S6). NH_4^+ concentrations are

428   also affected by the gas-particle partitioning equilibrium, and decease as the pH value gets higher (or

429   increase with H^+ concentrations). Therefore, the competition between the N_2O_5 – $ClNO_2$ chemistry and

430   N_2O_5 hydrolysis could also affect the formation of NH_4^+. In other words, increased Cl^- concentrations

431   could results in less H^+ and thus less NH_4^+. Consequently, there also exits some decrease in NH_4^+

432   concentrations in the SCB associated with the large decrease in NO_3^- concentrations. In contrast, little

433   change is found for surface SO_4^{2-} concentrations, less than 0.5 µg m^{-3} in most regions of China (Fig. S6).

434   It is worth mentioning that the effects of the additional chlorine emissions work mainly through the N_2O_5

435   – $ClNO_2$ chemistry. Without this heterogeneous chemistry, the increase of chlorine emissions shows only

436   a minor change in Cl atoms (< 10^3 molec cm^{-3} in China, estimated as the difference between the NoHet

437   and NoEmHet cases in Fig. S7). The impact of chlorine emissions on O_3 concentrations also weakens

438   when the N_2O_5 – $ClNO_2$ chemistry is turned off, with an increase of 0.5 – 1 ppbv in MDA8 O_3 on annual

439   average (vs. 0.5 – 3 ppbv mentioned above).

440   On the other hand, the impacts of N_2O_5 – $ClNO_2$ chemistry on air quality in inland China would be

441   seriously underestimated if the additional anthropogenic and biomass burning chlorine sources are

442   ignored. If only seas salt chlorine emission is included in the simulation, the increase of $ClNO_2$ surface

443   concentrations resulted from N_2O_5 – $ClNO_2$ chemistry only occurs in coastal regions due to the

444   heterogeneous uptake of N_2O_5 on sea salt chloride aerosols (by up to 260 pptv on annual average,

445   indicated by the difference between the NoEm and NoEmHet cases, Fig. S8). Consequently, the increase

446   in Cl atoms and MDA8 O_3 surface concentrations is found mainly in coastal regions. For instance, annual

447   mean MDA8 O_3 concentrations are increased by up to 2 ppbv in coastal regions, but by less than 0.5

448   ppbv in inland China. In other words, the dominance of N_2O_5 – $ClNO_2$ chemistry in the impact of chlorine

449   chemistry on air quality in China is to large extent driven by the additional chlorine emissions.

450   **3.4 The effect of N_2O_5 – $ClNO_2$ chemistry in response to parameterizations for γ_{N2O5} and φ_{ClNO2}**

451   It should be noted that the impact of N_2O_5 – $ClNO_2$ chemistry on air quality not only depends on the

452   amount of chlorine emissions, but is also sensitive to the parameterizations for γ_{N2O5} and φ_{ClNO2}. As

453   discussed earlier (Fig. 3a), there exists a large difference in simulated N_2O_5 between the Base and NoEm

454   cases at the Wangdu site, implying the sensitivity of γ_{N2O5} to chlorine emissions in the Yu

455   parameterization and thus the importance of non-sea salt chlorine emissions in inland China. The

456   comparison between the Base and NoHet cases (not shown here) also suggests that the heterogeneous

457   uptake of N_2O_5 on chloride-containing aerosol surfaces in the Yu Parameterization is an important loss

458   pathway of N_2O_5, and should not be ignored.

459   In contrast, N_2O_5 concentrations have little dependence on chlorine emissions in the McDuffie

460   parameterization (Fig. 3a). This insensitivity to chlorine emissions could be expected from Eq. 1 where

461   γ_{N2O5} relies mainly on total concentrations of inorganic species, of which chlorine is only a minor

462   component. The smaller dependence of γ_{N2O5} on concentrations of Cl^- together with the lower value of

463   φ_{ClNO2} make the results from the McDuffie case less sensitive to chlorine emissions, producing less

464    $ClNO_2$ and Cl atoms compared with the Base case (Yu parameterization) although with the same emission.

465   Consequently the McDuffie case produces less O_3, with annual mean surface concentrations of MDA8

466   O_3 lower by 0.47 ppbv averaged in China (by up to 2 ppbv in the SCB), but results in more $PM_{2.5}$ (0.63

467    $\mu g\ m^{-3}$ averaged in China and up to 4.7 $\mu g\ m^{-3}$ in the SCB on annual mean basis) mainly due to NO_3^- (Fig.

468   8). In other words, compared to the Base case with the Yu parameterization, the impacts of chlorine

469   emissions on annual MDA8 O_3 and $PM_{2.5}$ in the McDuffie case has been decreased by 48% and 27%

470   averaged in China, respectively. Therefore, even with the same amounts of emissions, the impacts of

471   N_2O_5 – $ClNO_2$ chemistry on air quality varies significantly with different parameterizations.

472   **4 Conclusions**

473   Considering the importance of chlorine chemistry in modulating the O_3 and $PM_{2.5}$ as well as the

474   previously ignored chlorine emission from anthropogenic and biomass burning, we updated the GOES-

475   Chem model in this study with comprehensive chlorine emissions and a new parameterization based on

476   the study of Yu et al. (2020) for N_2O_5 – $ClNO_2$ chemistry, followed by the extensive evaluation of model

477   performance. Through the utilization of a large number of observational datasets, we found a substantial

478   improvement has been achieved by the additional chlorine emissions, with NMB decreasing from -96%

479   – -79% to -36% – 39% for Cl^- simulation. The comparison with observed N_2O_5 and $ClNO_2$ also indicates

480   better model performance with Yu parameterization while γ_{N2O5} and φ_{ClNO2} are underestimated in

481   McDuffie parameterization (a default setting in GEOS-Chem), resulting in larger model bias. The

482   simulation of O_3 and $PM_{2.5}$ also agrees better with observations in general in the Base case (with the

483   additional chlorine emissions and Yu parameterization) than the others.

484   Total tropospheric chlorine chemistry could increase Cl atoms by up to 7×10^3 molec cm^{-3}, and leads to

485   an increase of up to 4.5 ppbv in MDA8 O_3 but a decrease of up to 7.9 μg m^{-3} in $PM_{2.5}$ concentrations on

486   an annual mean basis in China. The decrease in $PM_{2.5}$ is mainly associated with the decrease in NO_3^- and

487   NH_4^+, by up to 6.4 and 1.9 μg m^{-3}, respectively. The results also indicate that the N_2O_5 – $ClNO_2$ chemistry

488   dominate the impact of chlorine chemistry, accounting for 83% and 90% of total change in O_3 and $PM_{2.5}$

489   concentrations. In other words, the chlorine chemistry without the N_2O_5 – $ClNO_2$ chemistry has a minor

490   effect on annual mean MDA8 O_3 (less than 0.7 ppbv) and $PM_{2.5}$ (less than 1.5 μg m^{-3}) concentrations in

491   China. This mechanism is particularly useful in elucidating the commonly seen O_3 underestimations (e.g.

492   Ma et al. (2019)).

493   The effect of N_2O_5 – $ClNO_2$ chemistry is sensitive to chlorine emissions. With the additional

494   anthropogenic and biomass burning sources, simulated $PM_{2.5}$ concentrations are increased by up to 4.5

495    $\mu g\ m^{-3}$ in the NCP but decreased by up to 3.7 $\mu g\ m^{-3}$ in the SCB on an annual basis. The latter is mainly

496   driven by the decrease of NO_3^- due to the competition between the formation of $ClNO_2$ and HNO_3 upon

497   the uptake of N_2O_5 on aerosol surfaces. The additional emissions also increase Cl atoms and OH in China

498   associated with the photolysis of $ClNO_2$, consequently leading to an increase of annual mean MDA8 O_3

499   concentrations by up to 3.5 ppbv. In contrast, the significance of the $N_2O_5 - ClNO_2$ chemistry especially

500   over inland China would be severely underestimated if only sea salt chlorine is considered, with only a

501   slight increase in MDA8 O_3 (< 0.5 ppbv) and a minor decrease in $PM_{2.5}$ (< 1.5 $\mu g\ m^{-3}$) in inland China.

502   Moreover, we found the importance of chlorine chemistry not only depends on the amount of emissions,

503   but is also sensitive to the parameterizations for $N_2O_5 - ClNO_2$ chemistry. Although with the same

504   emission, the effects on MDA8 O_3 and $PM_{2.5}$ in China from the McDuffie case are lower compared to

505   the results with the Yu parameterization: differing by 48% and 27% in the annual average, respectively.

506   **Acknowledgements**

507   This study is supported by the National key R&D Program of China (2018YFC0213901), the National

508   Natural Science Foundation of China (41907182, 41877303, 91644218, 41877302, 41875156), the

509   Fundamental Research Funds for the Central Universities (21621105), Guangdong Natural Science

510   Funds for Distinguished Young Scholar (grant No. 2018B030306037), the Guangdong Innovative and

511   Entrepreneurial Research Team Program (Research team on atmospheric environmental roles and

512   effects of carbonaceous species: 2016ZT06N263), and Special Fund Project for Science and

513   Technology Innovation Strategy of Guangdong Province (2019B121205004).

514   **Competing interests.**

515   The authors declare that they have no conflict of interest.

516   **Data availability**

517   The data used in this study are available upon request from Qiaoqiao Wang (qwang@jnu.edu.cn).

518   **References**

519   Atkinson, R., Baulch, D. L., Cox, R. A., Crowley, J. N., Hampson, R. F., Hynes, R. G., Jenkin, M. E.,
520   Rossi, M. J., Troe, J., and Subcommittee, I.: Evaluated kinetic and photochemical data for
521   atmospheric chemistry: Volume II - gas phase reactions of organic species, Atmos. Chem. Phys., 6,
522   3625-4055, 10.5194/acp-6-3625-2006, 2006.

523   Bertram, T. H. and Thornton, J. A.: Toward a general parameterization of N2O5 reactivity on aqueous
524   particles: the competing effects of particle liquid water, nitrate and chloride, Atmospheric Chemistry
525   & Physics Discussions, 9, 191-198, 2009.

526   Chang, W. L., Brown, S. S., Stutz, J., Middlebrook, A. M., Bahreini, R., Wagner, N. L., Dubé, W. P.,
527   Pollack, I. B., Ryerson, T. B., and Riemer, N.: Evaluating N2O5 heterogeneous hydrolysis
528   parameterizations for CalNex 2010, J. Geophys. Res.: Atmos., 121, 5051-5070,
529   https://doi.org/10.1002/2015JD024737, 2016.

530   Chen, C., Zhang, H., Yan, W., Wu, N., Zhang, Q., and He, K.: Aerosol water content enhancement leads
531   to changes in the major formation mechanisms of nitrate and secondary organic aerosols in winter
532   over   the   North   China   Plain,   Environ.   Pollut.,   287,   117625,
533   https://doi.org/10.1016/j.envpol.2021.117625, 2021a.

534   Chen, W., Ye, Y., Hu, W., Zhou, H., Pan, T., Wang, Y., Song, W., Song, Q., Ye, C., Wang, C., Wang, B.,
535   Huang, S., Yuan, B., Zhu, M., Lian, X., Zhang, G., Bi, X., Jiang, F., Liu, J., Canonaco, F., Prevot,
536   A. S. H., Shao, M., and Wang, X.: Real-Time Characterization of Aerosol Compositions, Sources,
537   and Aging Processes in Guangzhou During PRIDE-GBA 2018 Campaign, J. Geophys. Res.: Atmos.,
538   126, e2021JD035114, https://doi.org/10.1029/2021JD035114, 2021b.

539   Choi, M. S., Qiu, X., Zhang, J., Wang, S., Li, X., Sun, Y., Chen, J., and Ying, Q.: Study of Secondary
540   Organic Aerosol Formation from Chlorine Radical-Initiated Oxidation of Volatile Organic
541   Compounds in a Polluted Atmosphere Using a 3D Chemical Transport Model, Environ. Sci.
542   Technol., 54, 13409-13418, 10.1021/acs.est.0c02958, 2020.

543   Dai, J., Liu, Y., Wang, P., Fu, X., Xia, M., and Wang, T.: The impact of sea-salt chloride on ozone through
544   heterogeneous reaction with N2O5 in a coastal region of south China, Atmos. Environ., 236, 117604,
545   https://doi.org/10.1016/j.atmosenv.2020.117604, 2020.

546   DeCarlo, P. F., Kimmel, J. R., Trimborn, A., Northway, M. J., Jayne, J. T., Aiken, A. C., Gonin, M., Fuhrer,

547   K., Horvath, T., Docherty, K. S., Worsnop, D. R., and Jimenez, J. L.: Field-Deployable, High-
548   Resolution, Time-of-Flight Aerosol Mass Spectrometer, Anal. Chem., 78, 8281-8289,
549   10.1021/ac061249n, 2006.

550   Finlayson-Pitts, B. J., Ezell, M. J., and Pitts, J. N. J.: Formation of chemically active chlorine compounds
551   by reactions of atmospheric NaCl particles with gaseous N2O5 and ClONO2, Cheminform, 20, 241-
552   244, 1989.

553   Fountoukis, C. and Nenes, A.: ISORROPIA II: a computationally efficient thermodynamic equilibrium
554   model for $K^+–Ca^{2+}–Mg^{2+}–NH_4^+–Na^+–SO_4^{2-}–NO_3^-–Cl^-–H_2O$ aerosols, Atmos. Chem. Phys., 7, 4639-
555   4659, 10.5194/acp-7-4639-2007, 2007.

556   Fu, X., Wang, T., Wang, S., Zhang, L., Cai, S., Xing, J., and Hao, J.: Anthropogenic Emissions of
557   Hydrogen Chloride and Fine Particulate Chloride in China, Environ. Sci. Technol., 52, 1644, 2018.

558   Geng, G., Zhang, Q., Martin, R. V., Van Donkelaar, A., Huo, H., Che, H., Lin, J., and He, K.: Estimating
559   long-term PM2.5 concentrations in China using satellite-based aerosol optical depth and a chemical
560   transport model, Remote Sens. Environ., 166, 262-270, 2015.

561   Guenther, A., Karl, T., Harley, P., Wiedinmyer, C., Palmer, P. I., and Geron, C.: Estimates of global
562   terrestrial isoprene emissions using MEGAN (Model of Emissions of Gases and Aerosols from
563   Nature), Atmos. Chem. Phys., 6, 3181-3210, 10.5194/acp-6-3181-2006, 2006.

564   Haskins, J. D., Lee, B. H., Lopez-Hilifiker, F. D., Peng, Q., Jaeglé, L., Reeves, J. M., Schroder, J. C.,
565   Campuzano-Jost, P., Fibiger, D., McDuffie, E. E., Jiménez, J. L., Brown, S. S., and Thornton, J. A.:
566   Observational Constraints on the Formation of Cl2 From the Reactive Uptake of ClNO2 on Aerosols
567   in the Polluted Marine Boundary Layer, J. Geophys. Res.: Atmos., 124, 8851-8869,
568   https://doi.org/10.1029/2019JD030627, 2019.

569   Hong, Y., Liu, Y., Chen, X., Fan, Q., Chen, C., Chen, X., and Wang, M.: The role of anthropogenic
570   chlorine emission in surface ozone formation during different seasons over eastern China, Sci. Total
571   Environ., 723, 137697, https://doi.org/10.1016/j.scitotenv.2020.137697, 2020.

572   Hossaini, R., Chipperfield, M. P., Saiz-Lopez, A., Fernandez, R., Monks, S., Feng, W., Brauer, P., and
573   von Glasow, R.: A global model of tropospheric chlorine chemistry: Organic versus inorganic
574   sources and impact on methane oxidation, J. Geophys. Res.: Atmos., 121, 14,271-214,297,
575   https://doi.org/10.1002/2016JD025756, 2016.

576   Huang, Z., Zhong, Z., Sha, Q., Xu, Y., Zhang, Z., Wu, L., Wang, Y., Zhang, L., Cui, X., Tang, M., Shi,
577   B., Zheng, C., Li, Z., Hu, M., Bi, L., Zheng, J., and Yan, M.: An updated model-ready emission
578   inventory for Guangdong Province by incorporating big data and mapping onto multiple chemical
579   mechanisms, Sci. Total Environ., 769, 144535, https://doi.org/10.1016/j.scitotenv.2020.144535,
580   2021.

581 Jaeglé, L., Quinn, P. K., Bates, T. S., Alexander, B., and Lin, J. T.: Global distribution of sea salt aerosols:
582   new constraints from in situ and remote sensing observations, Atmos. Chem. Phys., 11, 3137-3157,
583   10.5194/acp-11-3137-2011, 2011.

584 Kercher, J. P., Riedel, T. P., and Thornton, J. A.: Chlorine activation by N2O5: simultaneous, in situ
585   detection of ClNO2 and N2O5 by chemical ionization mass spectrometry, Atmospheric
586   Measurement Techniques Discussions, 2009.

587 Lawler, M. J., Sander, R., Carpenter, L. J., Lee, J. D., and Saltzman, E. S.: HOCl and Cl2 observations
588   in marine air, Atmos. Chem. Phys., 11, 8115-8144, 10.5194/acp-11-7617-2011, 2011.

589 Le Breton, M., Hallquist, Å. M., Pathak, R. K., Simpson, D., Wang, Y., Johansson, J., Zheng, J., Yang,
590   Y., Shang, D., Wang, H., Liu, Q., Chan, C., Wang, T., Bannan, T. J., Priestley, M., Percival, C. J.,
591   Shallcross, D. E., Lu, K., Guo, S., Hu, M., and Hallquist, M.: Chlorine oxidation of VOCs at a semi-
592   rural site in Beijing: Significant chlorine liberation from ClNO2 and subsequent gas and particle
593   phase Cl-VOC production, Atmos. Chem. Phys., 18, 13013-13030, 10.5194/acp-18-13013-2018,
594   2018.

595 Lee, B. H., Lopez-Hilfiker, F. D., Schroder, J. C., Campuzano-Jost, P., Jimenez, J. L., McDuffie, E. E.,
596   Fibiger, D. L., Veres, P. R., Brown, S. S., Campos, T. L., Weinheimer, A. J., Flocke, F. F., Norris, G.,
597   O'Mara, K., Green, J. R., Fiddler, M. N., Bililign, S., Shah, V., Jaeglé, L., and Thornton, J. A.:
598   Airborne Observations of Reactive Inorganic Chlorine and Bromine Species in the Exhaust of Coal-
599   Fired   Power   Plants,   J.   Geophys.   Res.: Atmos.,   123,   11,225-211,237,
600   https://doi.org/10.1029/2018JD029284, 2018.

601 Li, G., Su, H., Ma, N., Tao, J., Kuang, Y., Wang, Q., Hong, J., Zhang, Y., Kuhn, U., Zhang, S., Pan, X.,
602   Lu, N., Tang, M., Zheng, G., Wang, Z., Gao, Y., Cheng, P., Xu, W., Zhou, G., Zhao, C., Yuan, B.,
603   Shao, M., Ding, A., Zhang, Q., Fu, P., Sun, Y., Pöschl, U., and Cheng, Y.: Multiphase chemistry
604   experiment in Fogs and Aerosols in the North China Plain (McFAN): integrated analysis and
605   intensive winter campaign 2018, Faraday Discuss., 226, 207-222, 10.1039/D0FD00099J, 2021.

606 Li, K., Jacob, D. J., Liao, H., Shen, L., Zhang, Q., and Bates, K. H.: Anthropogenic drivers of 2013–2017
607   trends in summer surface ozone in China, P. Natl. Acad. Sci., 116, 422-427,
608   10.1073/pnas.1812168116, 2019.

609 Li, M., Zhang, Q., Kurokawa, J. I., Woo, J. H., He, K., Lu, Z., Ohara, T., Song, Y., Streets, D. G.,
610   Carmichael, G. R., Cheng, Y., Hong, C., Huo, H., Jiang, X., Kang, S., Liu, F., Su, H., and Zheng,
611   B.: MIX: a mosaic Asian anthropogenic emission inventory under the international collaboration
612   framework of the MICS-Asia and HTAP, Atmos. Chem. Phys., 17, 935-963, 10.5194/acp-17-935-
613   2017, 2017.

614 Li, Q., Zhang, L., Wang, T., Tham, Y. J., Ahmadov, R., Xue, L., Zhang, Q., and Zheng, J.: Impacts of
615   heterogeneous uptake of dinitrogen pentoxide and chlorine activation on ozone and reactive
616   nitrogen partitioning: improvement and application of the WRF-Chem model in southern China,

617   Atmos. Chem. Phys., 16, 14875-14890, 10.5194/acp-16-14875-2016, 2016.

618   Liu, X., Qu, H., Huey, L. G., Wang, Y., Sjostedt, S., Zeng, L., Lu, K., Wu, Y., Hu, M., Shao, M., Zhu, T.,
619   and Zhang, Y.: High Levels of Daytime Molecular Chlorine and Nitryl Chloride at a Rural Site on
620   the North China Plain, Environ. Sci. Technol., 51, 9588-9595, 10.1021/acs.est.7b03039, 2017.

621   Liu, Y., Fan, Q., Chen, X., Zhao, J., Ling, Z., Hong, Y., Li, W., Chen, X., Wang, M., and Wei, X.:
622   Modeling the impact of chlorine emissions from coal combustion and prescribed waste incineration
623   on tropospheric ozone formation in China, Atmos. Chem. Phys., 18, 2709-2724, 10.5194/acp-18-
624   2709-2018, 2018.

625   Lobert, J. M., Keene, W. C., Logan, J. A., and Yevich, R.: Global chlorine emissions from biomass
626   burning: Reactive Chlorine Emissions Inventory, J. Geophys. Res.: Atmos., 104, 8373-8389,
627   https://doi.org/10.1029/1998JD100077, 1999.

628   Ma, M., Gao, Y., Wang, Y., Zhang, S., Leung, L. R., Liu, C., Wang, S., Zhao, B., Chang, X., Su, H.,
629   Zhang, T., Sheng, L., Yao, X., and Gao, H.: Substantial ozone enhancement over the North China
630   Plain from increased biogenic emissions due to heat waves and land cover in summer 2017, Atmos.
631   Chem. Phys., 19, 12195-12207, 10.5194/acp-19-12195-2019, 2019.

632   McDuffie, E. E., Fibiger, D. L., Dubé, W. P., Lopez Hilfiker, F., Lee, B. H., Jaeglé, L., Guo, H., Weber,
633   R. J., Reeves, J. M., Weinheimer, A. J., Schroder, J. C., Campuzano-Jost, P., Jimenez, J. L., Dibb, J.
634   E., Veres, P., Ebben, C., Sparks, T. L., Wooldridge, P. J., Cohen, R. C., Campos, T., Hall, S. R.,
635   Ullmann, K., Roberts, J. M., Thornton, J. A., and Brown, S. S.: ClNO2 Yields From Aircraft
636   Measurements During the 2015 WINTER Campaign and Critical Evaluation of the Current
637   Parameterization, J. Geophys. Res.: Atmos., 123, 12,994-913,015,
638   https://doi.org/10.1029/2018JD029358, 2018a.

639   McDuffie, E. E., Fibiger, D. L., Dubé, W. P., Lopez-Hilfiker, F., Lee, B. H., Thornton, J. A., Shah, V.,
640   Jaeglé, L., Guo, H., Weber, R. J., Michael Reeves, J., Weinheimer, A. J., Schroder, J. C.,
641   Campuzano-Jost, P., Jimenez, J. L., Dibb, J. E., Veres, P., Ebben, C., Sparks, T. L., Wooldridge, P.
642   J., Cohen, R. C., Hornbrook, R. S., Apel, E. C., Campos, T., Hall, S. R., Ullmann, K., and Brown,
643   S. S.: Heterogeneous N2O5 Uptake During Winter: Aircraft Measurements During the 2015
644   WINTER Campaign and Critical Evaluation of Current Parameterizations, J. Geophys. Res.: Atmos.,
645   123, 4345-4372, https://doi.org/10.1002/2018JD028336, 2018b.

646   Mitroo, D., Gill, T. E., Haas, S., Pratt, K. A., and Gaston, C. J.: ClNO2 Production from N2O5 Uptake
647   on Saline Playa Dusts: New Insights into Potential Inland Sources of ClNO2, Environ. Sci. Technol.,
648   53, 7442-7452, 2019.

649   Morgan, W. T., Ouyang, B., Allan, J. D., Aruffo, E., Di Carlo, P., Kennedy, O. J., Lowe, D., Flynn, M. J.,
650   Rosenberg, P. D., Williams, P. I., Jones, R., McFiggans, G. B., and Coe, H.: Influence of aerosol
651   chemical composition on N_2O_5 uptake: airborne regional measurements in northwestern Europe,
652   Atmos. Chem. Phys., 15, 973-990, 10.5194/acp-15-973-2015, 2015.

653   Ng, N. L., Herndon, S. C., Trimborn, A., Canagaratna, M. R., Croteau, P. L., Onasch, T. B., Sueper, D.,
654   Worsnop, D. R., Zhang, Q., Sun, Y. L., and Jayne, J. T.: An Aerosol Chemical Speciation Monitor
655   (ACSM) for Routine Monitoring of the Composition and Mass Concentrations of Ambient Aerosol,
656   Aerosol Sci. Technol., 45, 780-794, 10.1080/02786826.2011.560211, 2011.

657   Osthoff, H. D., Roberts, J. M., Ravishankara, A. R., Williams, E. J., Lerner, B. M., Sommariva, R., Bates,
658   T. S., Coffman, D., Quinn, P. K., Dibb, J. E., Stark, H., Burkholder, J. B., Talukdar, R. K., Meagher,
659   J., Fehsenfeld, F. C., and Brown, S. S.: High levels of nitryl chloride in the polluted subtropical
660   marine boundary layer, Nat. Geosci., 1, 324-328, 10.1038/ngeo177, 2008.

661   Riedel, T. P., Bertram, T. H., Crisp, T. A., Williams, E. J., Lerner, B. M., Vlasenko, A., Li, S. M., Gilman,
662   J., De Gouw, J., and Bon, D. M.: Nitryl Chloride and Molecular Chlorine in the Coastal Marine
663   Boundary Layer, Environ. Sci. Technol., 46, 10463-10470, 2012.

664   Sarwar, G., Simon, H., Xing, J., and Mathur, R.: Importance of tropospheric ClNO2 chemistry across the
665   Northern Hemisphere, Geophys. Res. Lett., 2014.

666   Schmidt, J. A., Jacob, D. J., Horowitz, H. M., Hu, L., Sherwen, T., Evans, M. J., Liang, Q., Suleiman, R.
667   M., Oram, D. E., Le Breton, M., Percival, C. J., Wang, S., Dix, B., and Volkamer, R.: Modeling the
668   observed tropospheric BrO background: Importance of multiphase chemistry and implications for
669   ozone,   OH,   and   mercury,   J.   Geophys.   Res.:   Atmos.,   121,   11,819-811,835,
670   https://doi.org/10.1002/2015JD024229, 2016.

671   Sherwen, T., Evans, M. J. J., Sommariva, R., Hollis, L. D. J., Ball, S., Monks, P., Reed, C., Carpenter, L.,
672   Lee, J. D., and Forster, G.: Effects of halogens on European air-quality, Faraday Discuss., 200, 2017.

673   Sherwen, T., Schmidt, J. A., Evans, M. J., Carpenter, L. J., Großmann, K., Eastham, S. D., Jacob, D. J.,
674   Dix, B., Koenig, T. K., Sinreich, R., Ortega, I., Volkamer, R., Saiz-Lopez, A., Prados-Roman, C.,
675   Mahajan, A. S., and Ordóñez, C.: Global impacts of tropospheric halogens (Cl, Br, I) on oxidants
676   and composition in GEOS-Chem, Atmos. Chem. Phys., 16, 12239-12271, 10.5194/acp-16-12239-
677   2016, 2016.

678   Simmonds, P. G., Manning, A. J., Cunnold, D. M., McCulloch, A., O'Doherty, S., Derwent, R. G.,
679   Krummel, P. B., Fraser, P. J., Dunse, B., Porter, L. W., Wang, R. H. J., Greally, B. R., Miller, B. R.,
680   Salameh, P., Weiss, R. F., and Prinn, R. G.: Global trends, seasonal cycles, and European emissions
681   of dichloromethane, trichloroethene, and tetrachloroethene from the AGAGE observations at Mace
682   Head,   Ireland,   and   Cape   Grim,   Tasmania,   J.   Geophys.   Res.:   Atmos.,   111,
683   https://doi.org/10.1029/2006JD007082, 2006.

684   Staudt, S., Gord, J. R., Karimova, N. V., McDuffie, E. E., Brown, S. S., Gerber, R. B., Nathanson, G. M.,
685   and Bertram, T. H.: Sulfate and Carboxylate Suppress the Formation of ClNO2 at Atmospheric
686   Interfaces, ACS Earth and Space Chemistry, 3, 1987-1997, 10.1021/acsearthspacechem.9b00177,
687   2019.

688   Tian, M., Liu, Y., Yang, F., Zhang, L., Peng, C., Chen, Y., Shi, G., Wang, H., Luo, B., Jiang, C., Li, B.,
689   Takeda, N., and Koizumi, K.: Increasing importance of nitrate formation for heavy aerosol pollution
690   in two megacities in Sichuan Basin, southwest China, Environ. Pollut., 250, 898-905,
691   https://doi.org/10.1016/j.envpol.2019.04.098, 2019.

692   Van, d. W., G. R., Randerson, J. T., Giglio, L., Collatz, G. J., Mu, M., Kasibhatla, P. S., Morton, D. C.,
693   Defries, R. S., Jin, Y., and Van Leeuwen, T. T.: Global fire emissions and the contribution of
694   deforestation, savanna, forest, agricultural, and peat fires (1997–2009), Atmos. Chem. Phys., 10,
695   16153-16230, 10.5194/acp-10-11707-2010, 2010.

696   Wang, T., Tham, Y. J., Xue, L., Li, Q., Zha, Q., Wang, Z., Poon, S. C. N., Dubé, W. P., Blake, D. R.,
697   Louie, P. K. K., Luk, C. W. Y., Tsui, W., and Brown, S. S.: Observations of nitryl chloride and
698   modeling its source and effect on ozone in the planetary boundary layer of southern China, J.
699   Geophys. Res.: Atmos., 121, 2476-2489, https://doi.org/10.1002/2015JD024556, 2016.

700   Wang, X., Jacob, D. J., Fu, X., Wang, T., and Liao, H.: Effects of Anthropogenic Chlorine on PM 2.5 and
701   Ozone Air Quality in China, Environ. Sci. Technol., 54, 9908-9916, 2020.

702   Wang, X., Jacob, D. J., Eastham, S. D., Sulprizio, M. P., Zhu, L., Chen, Q., Alexander, B., Sherwen, T.,
703   Evans, M. J., Lee, B. H., Haskins, J. D., Lopez-Hilfiker, F. D., Thornton, J. A., Huey, G. L., and
704   Liao, H.: The role of chlorine in global tropospheric chemistry, Atmos. Chem. Phys., 19, 3981-4003,
705   10.5194/acp-19-3981-2019, 2019.

706   Wang, Y., Shen, L., Wu, S., Mickley, L., He, J., and Hao, J.: Sensitivity of surface ozone over China to
707   2000–2050 global changes of climate and emissions, Atmos. Environ., 75, 374-382, 2013.

708   Xia, M., Wang, W., Wang, Z., Gao, J., Li, H., Liang, Y., Yu, C., Zhang, Y., Wang, P., Zhang, Y., Bi, F.,
709   Cheng, X., and Wang, T.: Heterogeneous Uptake of N2O5 in Sand Dust and Urban Aerosols
710   Observed during the Dry Season in Beijing, Atmosphere, 10, 204, 2019.

711   Xu, Z., Liu, M., Zhang, M., Song, Y., Wang, S., Zhang, L., Xu, T., Wang, T., Yan, C., Zhou, T., Sun, Y.,
712   Pan, Y., Hu, M., Zheng, M., and Zhu, T.: High efficiency of livestock ammonia emission controls
713   in alleviating particulate nitrate during a severe winter haze episode in northern China, Atmos. Chem.
714   Phys., 19, 5605-5613, 10.5194/acp-19-5605-2019, 2019.

715   Yang, X., Wang, T., Xia, M., Gao, X., Li, Q., Zhang, N., Gao, Y., Lee, S., Wang, X., Xue, L., Yang, L.,
716   and Wang, W.: Abundance and origin of fine particulate chloride in continental China, Sci. Total
717   Environ., 624, 1041-1051, https://doi.org/10.1016/j.scitotenv.2017.12.205, 2018.

718   Ye, C., Yuan, B., Lin, Y., Wang, Z., Hu, W., Li, T., Chen, W., Wu, C., Wang, C., Huang, S., Qi, J., Wang,
719   B., Wang, C., Song, W., Wang, X., Zheng, E., Krechmer, J. E., Ye, P., Zhang, Z., Wang, X., Worsnop,
720   D. R., and Shao, M.: Chemical characterization of oxygenated organic compounds in the gas phase
721   and particle phase using iodide CIMS with FIGAERO in urban air, Atmos. Chem. Phys., 21, 8455-
722   8478, 10.5194/acp-21-8455-2021, 2021.

723   Yu, C., Wang, Z., Xia, M., Fu, X., Wang, W., Tham, Y. J., Chen, T., Zheng, P., Li, H., Shan, Y., Wang, X.,
724   Xue, L., Zhou, Y., Yue, D., Ou, Y., Gao, J., Lu, K., Brown, S. S., Zhang, Y., and Wang, T.:
725   Heterogeneous N2O5 reactions on atmospheric aerosols at four Chinese sites: improving model
726   representation of uptake parameters, Atmos. Chem. Phys., 20, 4367-4378, 10.5194/acp-20-4367-
727   2020, 2020.

728   Zhang, T., de Jong, M. C., Wooster, M. J., Xu, W., and Wang, L.: Trends in eastern China agricultural
729   fire emissions derived from a combination of geostationary (Himawari) and polar (VIIRS) orbiter
730   fire radiative power products, Atmos. Chem. Phys., 20, 10687-10705, 10.5194/acp-20-10687-2020,
731   2020.

732

733
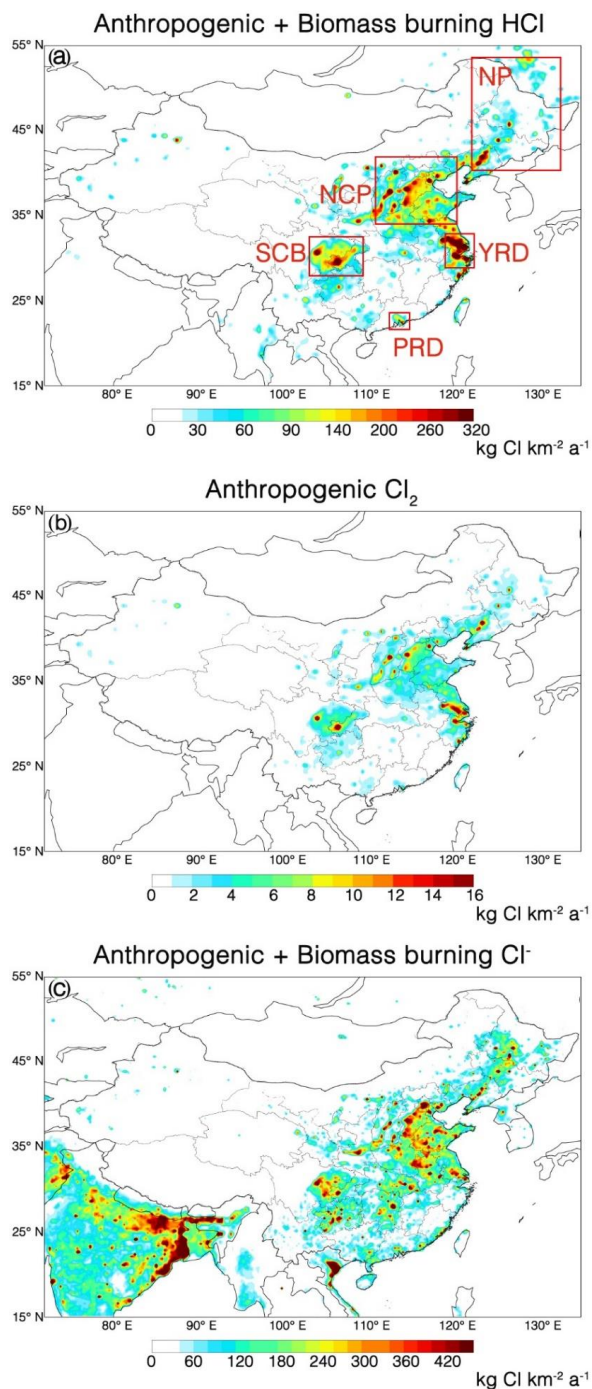
734 **Figure 1. Annual emissions of (a) HCl, (b) Cl₂, (c) non-sea salt Cl⁻.**

735

736
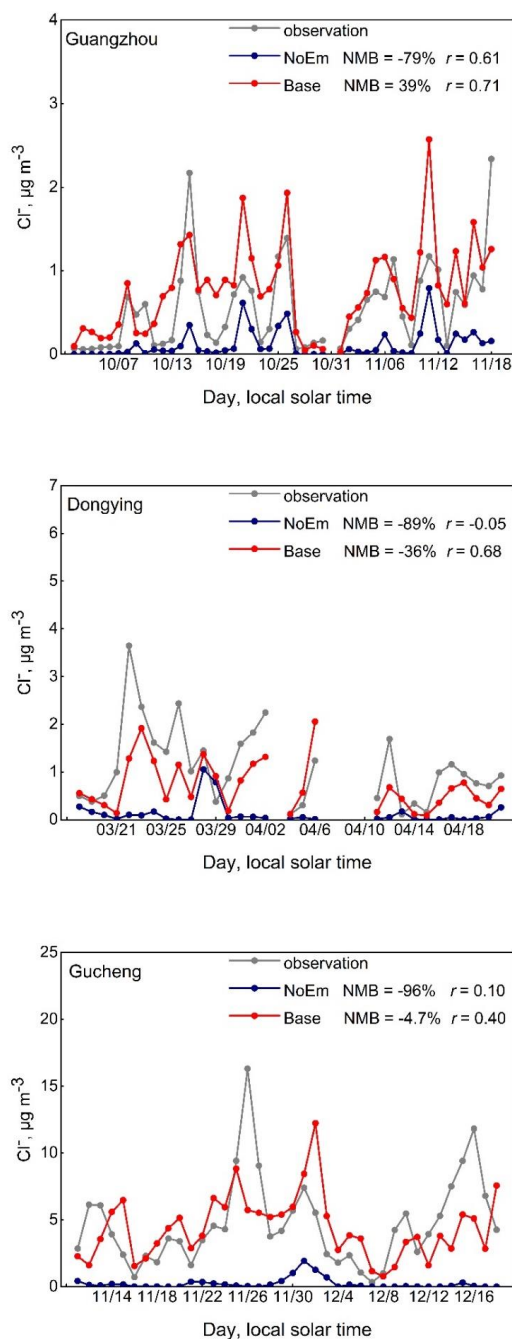
737 **Figure 2. Time series of simulated and observed particulate Cl⁻ concentrations at the Guangzhou, Dongying**

738 **and Gucheng sites.**

739
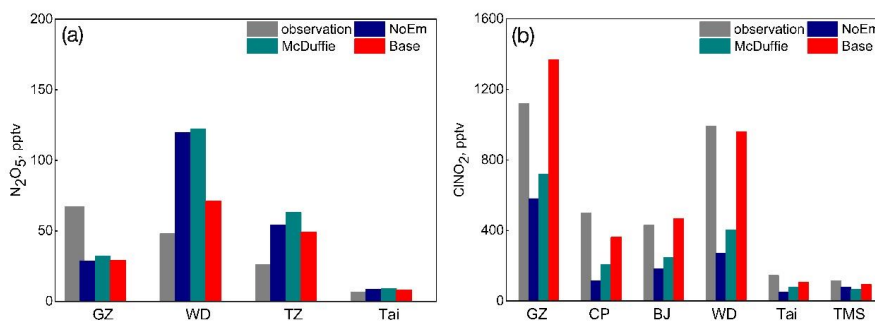
740

741   **Figure 3. Comparison of observed and simulated (a) averaged N_2O_5 concentrations and (b) mean nighttime**

742   **maximum mixing ratio of $ClNO_2$ concentrations at different sites. GZ: Guangzhou; WD: Wangdu; TZ:**

743   **Taizhou; Tai: Mount Tai; CP: Changping; BJ: Beijing; TMS: Mount TaiMoShan**

744
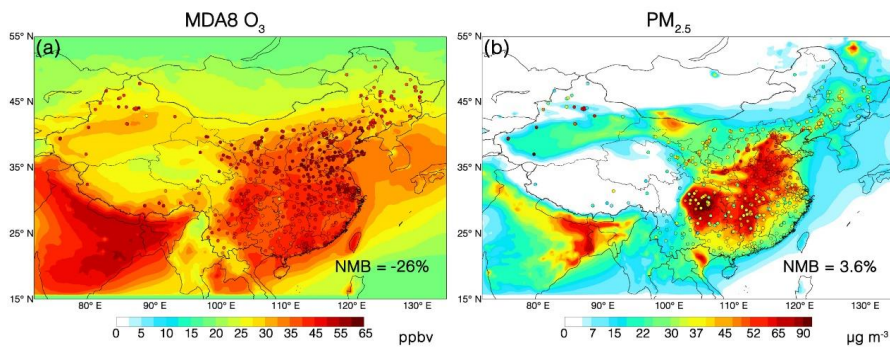
745

746   **Figure 4. Annual mean surface concentrations of (a) MDA8 O_3 and (b) $PM_{2.5}$ over China in 2018. GEOS-**

747   **Chem model values from the Base case are shown as contours. Observations from China National**

748   **Environmental Monitoring Center (CNEMC) are shown as circles.**

749

750
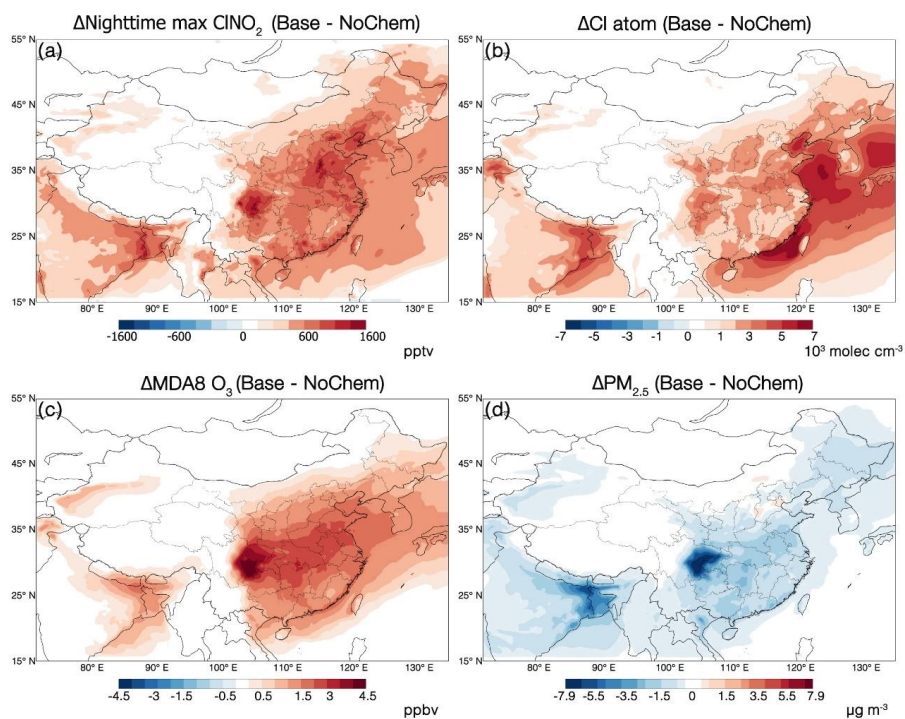
Figure 5. Effects of chlorine chemistry on annual mean surface concentrations of (a) nighttime max ClNO₂,

(b) Cl atom, (c) MDA8 O₃ and (d) PM₂.₅ in China, estimated as the differences between the Base and

NoChem cases.

755
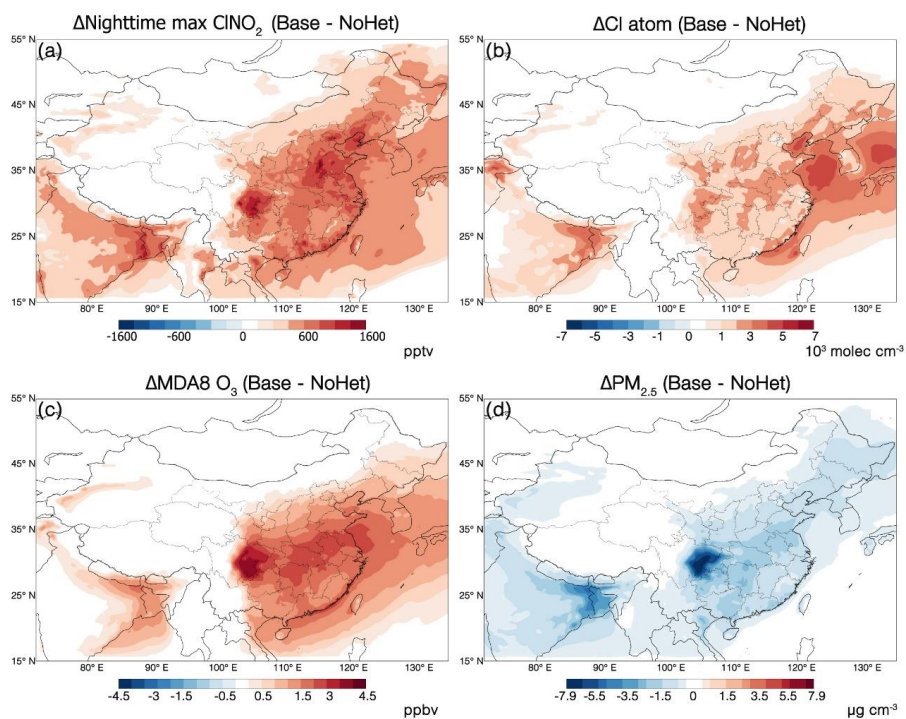
Figure 6. Effects of N₂O₅-ClNO₂ chemistry on annual mean surface concentrations of (a) nighttime max

756

ClNO₂, (b) Cl atom, (c) MDA8 O₃ and (d) PM₂.₅ in China, estimated as the differences between the Base and

757

NoHet cases.

758
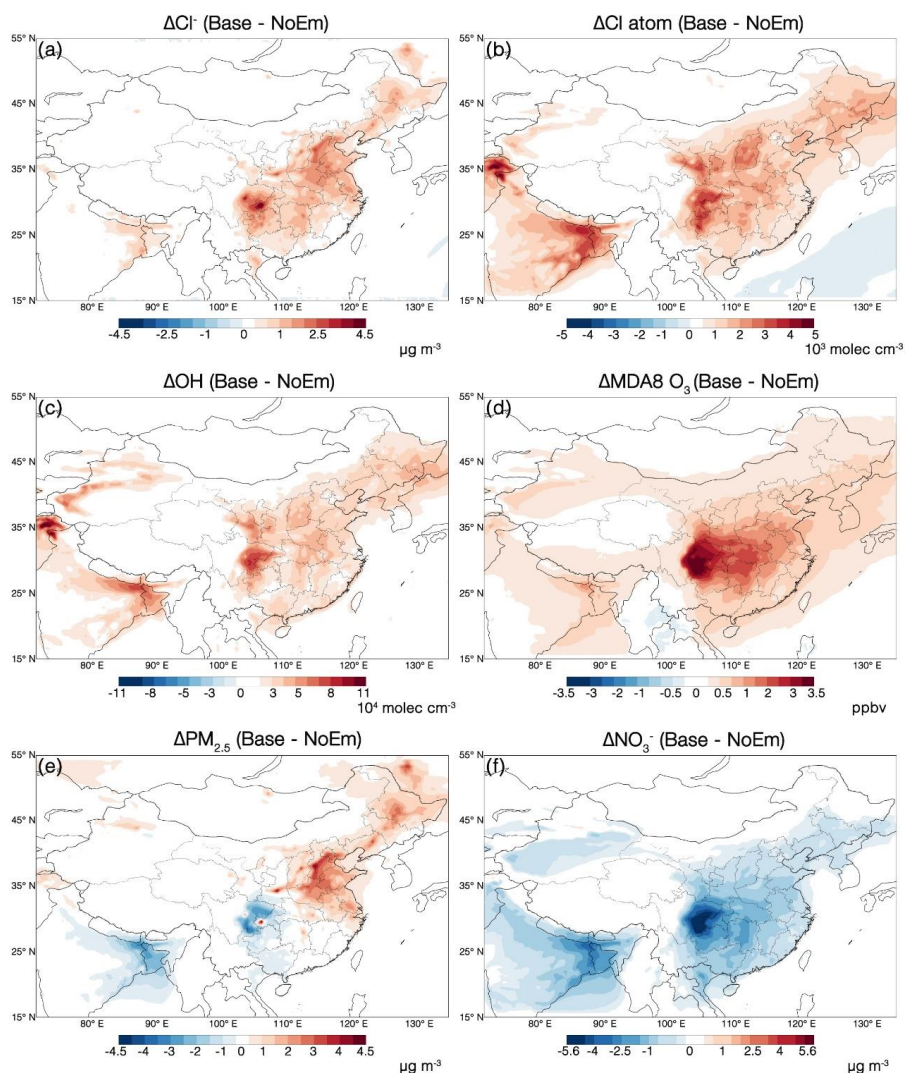
Figure 7. Effects of anthropogenic and biomass burning chlorine emissions on annual mean surface concentrations of (a) Cl⁻, (b) Cl atom, (c) OH, (d) MDA8 O₃, (e) PM₂.₅ and (f) NO₃⁻ in China, estimated as the differences between the Base and NoEm cases.
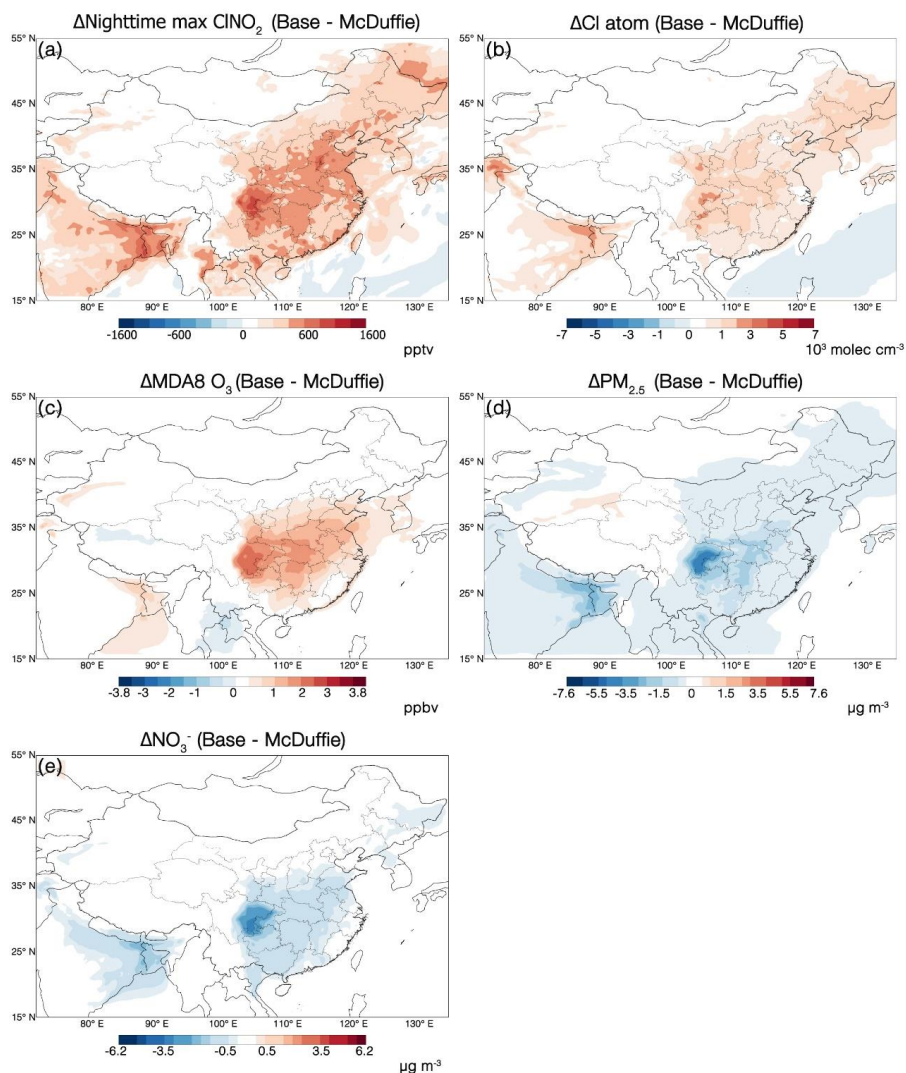
Figure 8. Effects of different parameterizations on annual mean surface concentrations of (a) nighttime max ClNO₂, (b) Cl atom, (c) MDA8 O₃, (d) PM₂.₅, and (e) NO₃⁻ in China, estimated as the differences between the Base and McDuffie cases.

776   **Table 1. Chlorine emissions in China in the model.**

Sources	By default (Gg Cl a^{-1})	Updated in this study (Gg Cl a^{-1})
Sea salt Cl$^-$	6.5×10^4	6.5×10^4
Anthropogenic HCl	0	218
Biomass burning HCl	0	30
Anthropogenic Cl$_2$	0	8.9
Anthropogenic Cl$^-$	0	379
Biomass burning Cl$^-$	0	120
CH$_3$Cl[a]	3.8	3.8
CH$_2$Cl$_2$[a]	2.4	2.4
CHCl$_3$[a]	0.70	0.70

777   [a]: Sources are shown in terms of the chemical release (e.g. +Cl, +OH, +hv)

778

779   **Table 2. Model setup of all simulation cases**

Cases	N$_2$O$_5$ uptake (γ_{N2O5})	ClNO$_2$ production (φ_{ClNO2})	Other tropospheric chlorine chemistry	Anthropogenic and biomass burning inorganic chlorine emissions
Base	Yu et al. (2020)	Yu et al. (2020)	Full	Yes
McDuffie	McDuffie et al. (2018a, 2018b)	McDuffie et al. (2018a, 2018b)	Full	Yes
NoEm	Yu et al. (2020)	Yu et al. (2020)	Full	None
NoHet	Yu et al. (2020) but with [Cl$^-$] = 0	None	Full	Yes
NoChem	Yu et al. (2020) but with [Cl$^-$] = 0	None	None	Yes
NoEmHet	Yu et al. (2020) but with [Cl$^-$] = 0	None	Full	None
NoAll	Yu et al. (2020) but with [Cl$^-$] = 0	None	None	None

780

781   **Table 3. Normalized mean bias (NMB) and correlation coefficients (*r*) between observed and simulated**

782   **MDA8 O$_3$ and PM$_{2.5}$ concentrations during 2018 in China**

Species	Time	Base NMB	Base *r*	McDuffie NMB	McDuffie *r*	NoEm NMB	NoEm *r*
MDA8 O$_3$	Annual	-26%	0.83	-27%	0.83	-28%	0.82
	MAM[a]	-35%	0.87	-36%	0.87	-36%	0.87
	JJA[b]	-5.5%	0.50	-5.2%	0.48	-5.9%	0.48
	SON[c]	-24%	0.79	-26%	0.78	-28%	0.76
	DJF[d]	-49%	0.81	-53%	0.8	-54%	0.80
PM$_{2.5}$	Annual	3.6%	0.81	5.6%	0.81	2.3%	0.80
	MAM	-6.3%	0.52	-4.9%	0.53	-6.2%	0.52
	JJA	3.9%	0.70	4.6%	0.70	5.0%	0.70
	SON	28%	0.79	32%	0.80	26%	0.79
	DJF	-4.3%	0.82	-2.6%	0.82	-7.9%	0.82

783   [a]: March, April, and May (Spring)

784   [b]: June, July, and August (Summer)

785   [c]: September, October, and November (Autumn)

786   [d]: December, January, and February (Winter)

787